



Contents lists available at ScienceDirect

Quaternary International

journal homepage: www.elsevier.com/locate/quaint

Late Holocene sea-level evolution of Paros Island (Cyclades, Greece)

Anna Karkani^{a,*}, Niki Evelpidou^a, Matthieu Giaime^b, Nick Marriner^c, Christophe Morhange^d,
Giorgio Spada^e

^a Faculty of Geology and Geoenvironment, National and Kapodistrian University of Athens, Panepistimiopolis, Zografou, 15784 Athens, Greece

^b University of Durham, Department of Geography, South Road, DH1 3LE, Durham, UK

^c CNRS, Laboratoire Chrono-Environnement UMR6249, Université de Franche-Comté, UFR ST, 16 Route de Gray, 25030 Besançon, France

^d Aix Marseille University, CNRS, IRD, Coll France, CEREGE, Aix-en-Provence, France; RIMS, The Leon Recanatì Institute for Maritime Studies University of Haifa, 31905, Israel

^e Dipartimento di Scienze Pure e Applicate (DiSPeA), Università di Urbino "Carlo Bo", Italy

ARTICLE INFO

Keywords:

Relative sea level
Subsidence
Coastal geomorphology
Lagoon
Holocene
Central Aegean

ABSTRACT

Relative sea-level (RSL) reconstructions are essential to answer a variety of scientific questions, ranging from the investigation of crustal movements to the calibration of earth rheology models and ice sheet reconstructions.

It is generally assumed that most Cycladic islands (Aegean Sea, Greece) are affected by a gradual subsidence, attributed to the crustal thinning and to hydro-isostatic processes that accompanied the post-glacial rise in sea level. In this paper, we produce new RSL data from sedimentary records on Paros Island. We compare and contrast these RSL data with published data from the nearby island of Naxos. Our results are further compared with sea-level predictions from two different GIA models in an attempt to better quantify the tectonic regime of the wider study area. Our results suggest average tectonic subsidence rates close to 1.0 ± 0.4 mm/yr since 5500 cal BP. These rates are not linear in time and have increased since 2500 cal BP.

1. Introduction

Sea-level changes are driven either by variations in the masses or volume of the oceans, defined as ‘eustatic’, or by changes of the land with respect to the sea surface, called ‘relative’ (Rovere et al., 2016). During the past 4000 years, the ice-equivalent melt-water input is considered minimal (Peltier, 2002; Milne et al., 2005; Church et al., 2008). Therefore, any significant changes in relative sea-level (RSL) are almost entirely driven by vertical land movements caused by tectonics and glacial isostatic adjustment (GIA) or sediment compaction (Engelhart et al., 2009; Teatini et al., 2011).

RSL reconstructions are key to probing various research questions, ranging from the calibration of earth rheology models and ice sheet reconstructions to the investigation of crustal movements (Lambeck et al., 2004; Peltier, 2004; Engelhart and Horton, 2012). GIA models have often been employed to identify stable and unstable areas and deduce tectonic rates through comparisons with observational data (e.g. Sivan et al., 2001, 2004; Pirazzoli, 2005; Pavlopoulos et al., 2011; Stiros et al., 2011; Van De Plassche et al., 2014; Woodroffe et al., 2015; Bradley et al., 2016; Chelli et al., 2017; Vacchi et al., 2017, 2018; Melis et al., 2018). Greece, like the rest of the Mediterranean, is characterized

by small tidal ranges that favor the preservation of sea level indicators (e.g. Rovere et al., 2012).

In this context, the main aim of this study is to elucidate the relative sea-level history of Paros island during the Late Holocene (i.e., last 4000 years), through the multiproxy analysis of a sediment core from the western part of the island, in combination with published data from the central Cyclades. We compare and contrast our results with new modelled curves for Paros island, in an attempt to reconstruct RSL changes and assess the tectonic regime of the central Cyclades.

2. Regional setting

The Cycladic Plateau has been subjected to successive stages of emergence and submergence due to changing sea level during the Quaternary (Kapsimalis et al., 2009). The central Aegean is considered to be an area of low seismicity, characterized by the absence of large earthquakes (Fig. 1) (e.g. Papazachos, 1990; Sakellariou and Galanidou, 2016). According to Sakellariou and Galanidou (2016), vertical tectonic movements are of minor significance and the coastal evolution of the central Aegean during Late Pleistocene-Holocene is mostly affected by eustatic sea-level fluctuations and, to a lesser degree, by isostatic

* Corresponding author.

E-mail addresses: ekarkani@geol.uoa.gr (A. Karkani), evelpidou@geol.uoa.gr (N. Evelpidou), matthieu.giaime@gmail.com (M. Giaime), nick.marriner@univ-fcomte.fr (N. Marriner), morhange@cerge.fr (C. Morhange), giorgio.spada@gmail.com (G. Spada).

<https://doi.org/10.1016/j.quaint.2019.02.027>

Received 26 November 2018; Received in revised form 14 February 2019; Accepted 18 February 2019

Available online 26 February 2019

1040-6182/ © 2019 Elsevier Ltd and INQUA. All rights reserved.

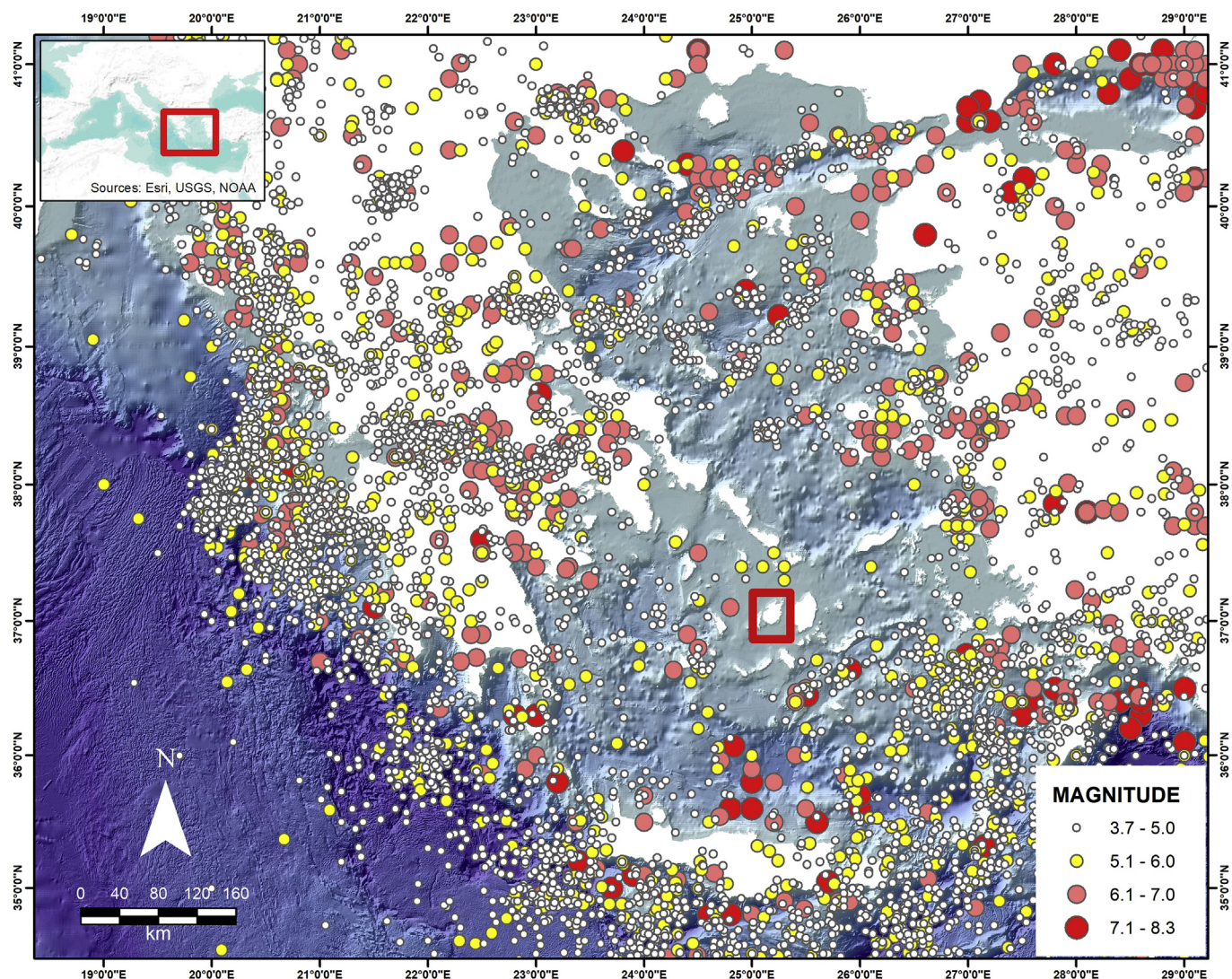


Fig. 1. Location of the study area and seismicity since 550 B.C. (seismicity data retrieved from http://geophysics.geo.auth.gr/ss/station_index_en.html). The red square denotes the location of Paros Island. The bathymetry was provided by EMODnet Bathymetry 2015. (For interpretation of the references to colour in this figure legend, the reader is referred to the Web version of this article.)

movements.

Lykousis (2009) noted a continuous subsidence rate during the last 400 ka, with values of 0.34–0.60 mm/yr for the Cycladic plateau, with a gradual decrease in the magnitude of the extensional tectonic regime. According to Tirel et al. (2004), the Cyclades probably act as a rigid block translated toward the south–west with no significant deformation, in agreement with GPS velocities and a lack of major earthquakes.

The island of Paros lies in the central Aegean Sea, constituting the third largest island in the Cyclades archipelago (Figs. 1 and 2). Paros forms a NE–SW trending dome bounded by a low-angle inactive normal fault to the east and northeast (Bargnesi et al., 2013). It has a rocky coastal zone, particularly in the northern part, characterized by the alternation of carbonate rocks, gneisses-schists and alluvial deposits (Papanikolaou, 1996). Beaches form a smaller part of coastal zone, mainly near coastal plains in the eastern part of the island.

The coring site, Pounta (POU2) is located in the western coast of Paros (Fig. 2a). POU2 core was drilled on the southwest coast, 1 km south of Pounta (Fig. 2a and b). Today, the area is characterized by the presence of coastal dunes, forming a sandy spit/barrier that frames a leeward lagoon.

3. Materials and methods

3.1. Palaeoenvironmental reconstruction

A borehole was drilled with a portable drilling sampler, 35 mm in diameter, reaching a maximum depth of 4 m below mean sea level (msl). For the palaeoenvironmental reconstruction, multiproxy analyses were undertaken, which included sedimentological analysis of the core, biostratigraphy of the macrofauna and ostracods and radiocarbon dating.

The core was analyzed at Chrono-environment (CNRS, University of Franche-Comté, Besançon, France). The core was first studied and photographed in detail in order to record the general stratigraphy. The sediment texture was determined by separating out the gravel (> 2 mm), sand (2 mm–50 μ m) and silt/clay (< 50 μ m) fractions, using two sieve mesh sizes, 2 mm and 50 μ m.

The gravel fraction of the sediments was examined to identify mollusc shells and determine their ecology. The identifications and classifications are based on d' Angelo and Gargiullo (1978) and Doneddu and Trainito (2005). The species were assigned to ecological groups defined by Pérès and Picard (1964) and Pérès (1982). Ostracods were extracted from the dry sand fraction (> 150 μ m). The identified

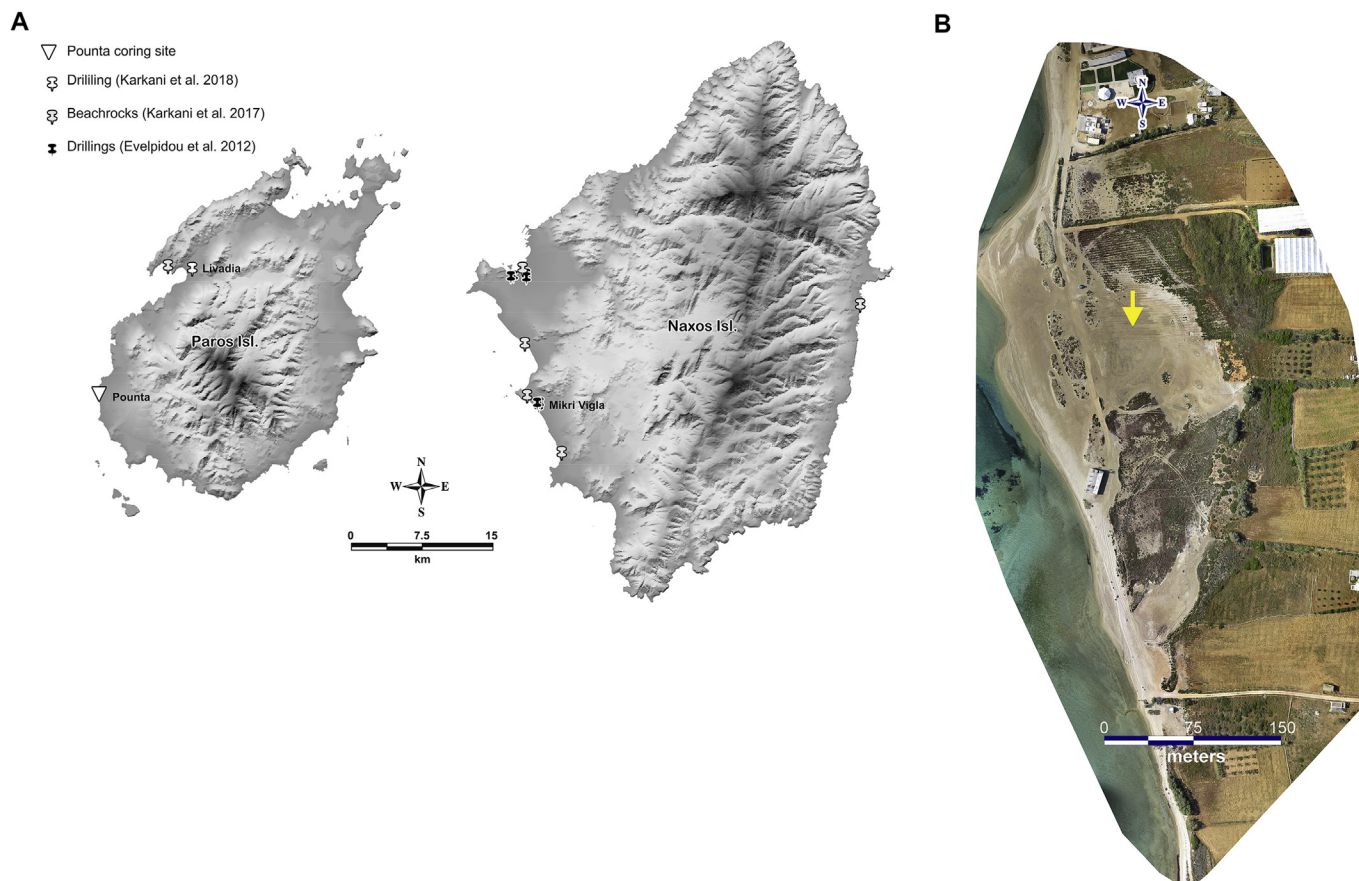


Fig. 2. a) Location of the drilling site on Paros Island and sea-level data used in this study from Evelpidou et al. (2012) and Karkani et al. (2017, 2018), b) Aerial view of Pounta coring site.

Table 1

Radiocarbon ages for dated samples from the Paros core. The data were calibrated using the online software Calib 7.10 (Stuiver et al., 2016) with the Marine13 curve (Reimer et al., 2013). Shell samples were corrected for the local marine reservoir effect according to Reimer and McCormac (2002), using a mean ΔR value of 154 ± 52 for the Aegean Sea.

Sample code	Lab code	Depth below sea level (m)	Material	$\delta^{13}\text{C}$	^{14}C BP	Age cal. BP	Cal. BC/AD (2σ)
POU2-1	Poz-81147	85	Conus mediterraneus	2.8	520 ± 30	–	–
POU2-2	Poz-81148	186–196	Loripes lacteus	0.3	715 ± 30	40–298	1652–1910 AD
POU2-3	Poz-81354	260–270	Cerithium vulgatum	–3.9	1475 ± 30	721–986	964–1229 AD
POU2-4	Poz-81140	337–346	Nassarius louisi	4.9	490 ± 30	–	–

taxa were assigned to assemblages based on their ecological preferences: freshwater, lagoonal, marine lagoonal, coastal and marine (Lachenal, 1989; Nachite et al., 2010; Salel et al., 2016).

3.2. Chronology

The chronostratigraphy of the core is based on four AMS radiocarbon dates performed at the Poznan Radiocarbon Laboratory (Poland) (Table 1). The radiocarbon ages of the samples were calibrated using the online software Calib 7.10 (Stuiver et al., 2016) with the Marine13 curve (Reimer et al., 2013). Ages of the shell samples were corrected for the local marine reservoir effect according to Reimer and McCormac (2002), using a mean ΔR value of 154 ± 52 for the Aegean Sea.

3.3. Sea-level reconstruction

Results of the paleo-environmental reconstruction of the new core revealed facies characteristic of coastal and lagoonal environments. We

produced a new suite of RSL index points following the protocol developed by Vacchi et al. (2016), which has been used in a number of recent Mediterranean studies (e.g. Vacchi et al., 2017, 2018; Karkani et al., 2017; Fontana et al., 2017; Melis et al., 2017, 2018). The indicative meaning of each index point is composed of a reference water level (RWL) and the indicative range (IR). The IR corresponds to the elevation interval over which an indicator is formed and the RWL is the midpoint of this range, expressed relative to the same datum as the elevation of the sampled indicator (e.g. Horton and Shennan, 2009; Gehrels and Woodworth, 2013; Hijma et al., 2015).

For the production of RSL index points from the core, we attributed an indicative range from 0 to -2 m for samples found in an open or marine-influenced lagoon and an indicative range from 0 to -1 m for an inner or semi-enclosed lagoon (Vacchi et al., 2016). Although no modern analogues have been reported in the literature for the study area, the indicative ranges reported by Vacchi et al. (2016) have been adopted considering the geomorphological status of the coastal lagoons in the Cyclades. More precisely, in the Cycladic area, and on Paros in particular, the contemporary coastal lagoons are usually dry during the

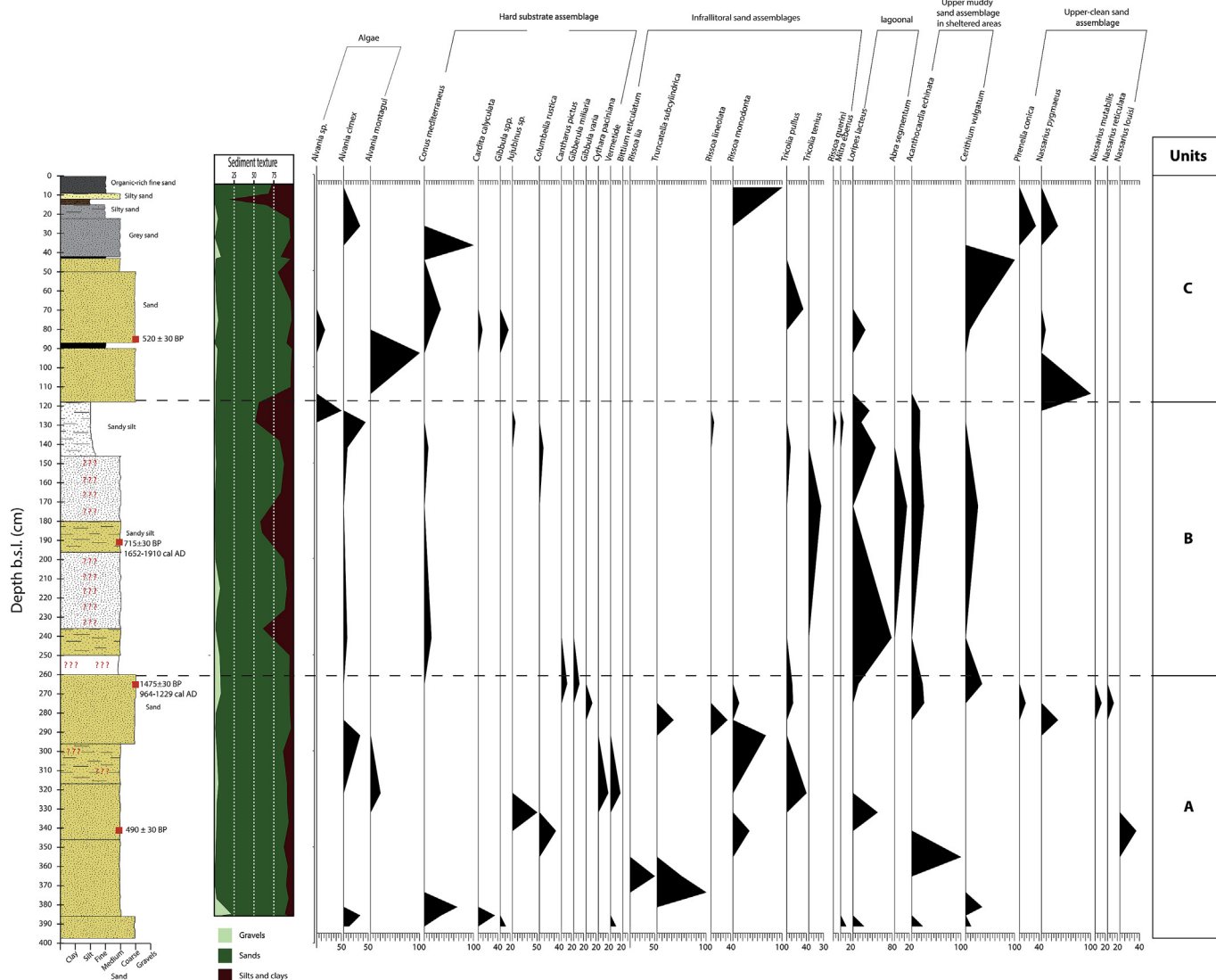


Fig. 3. Core POU2 stratigraphy and macrofauna.

summer while, during winter, their depths do not exceed 1–2 m. We added additional vertical errors to each index point, including: a) an error of ± 0.2 m for the samples altitude and b) a core stretching/shortening error of 0.15m (Hijma et al., 2015).

RSL index points were further produced using samples deposited in semi-enclosed lagoon facies from Evelpidou et al. (2012) and from Karkani et al. (2018), and from samples found in a brackish environment, most likely deposited within ± 0.5 m of former MSL (Pavlopoulos et al., 2011; Evelpidou et al., 2012; Karkani et al., 2017) (Fig. 2a). We further took into consideration the beachrock luminescence dating results from Karkani et al. (2017) for Paros and Naxos (Fig. 2a). Various studies in the eastern Mediterranean have shown that beachrocks are accurate sea-level indicators, as long as they are supported by cement mineralogy and morphology and, if possible, by sedimentary information (e.g. Desruelles et al., 2009; Mauz et al., 2015). The dated beachrock samples of the study area showed clear intertidal formation based on cement characteristics and therefore an indicative range between the Mean High Tide (MHT) and Mean Low Tide (MLT) (i.e. 0.14 m; HNHS, 2012) was considered (Karkani et al., 2017).

To interpret the observational RSL data, we considered predictions from two Glacial Isostatic Adjustment (GIA) models. The first is ICE-6G (VM5a) of Peltier et al. (2015) while the second (ANU), is the latest version of the GIA model progressively developed by K. Lambeck and

co-workers (see Lambeck et al., 2003 and further refinements). For both GIA models, we solved the Sea Level Equation using an improved version of the program SELEN (Spada and Stocchi, 2007), in which the horizontal migration of shorelines, the transition between grounded and floating ice and the rotational feedback on sea-level are taken into account. The two GIA models are characterized by different chronologies for the melting of the late-Pleistocene ice sheets but also different rheological profiles. In particular, while in ICE-6G (VM5a) the lower mantle viscosity is $3.2 \cdot 10^{21}$ Pa s, for ANU we adopted a value 10^{22} Pa s, in the range suggested in the study of Lambeck et al. (2017). The relatively high lower mantle viscosity in ANU compared to ICE-6G (VM5a) generally implies a larger isostatic disequilibrium and higher rates of glacial-isostatic readjustment during the last few millennia, consistent with the results below.

4. Results

4.1. Lithology-faunal evidence - depositional environment

4.1.1. Unit A: shallow marine environment

Unit A, from the bottom of the core (4 m) up to 2.6 m b.s.l. is dominated by medium to coarse sands with shell fragments (Figs. 3 and 4). The sand fraction comprises more than 87% of the total sediment

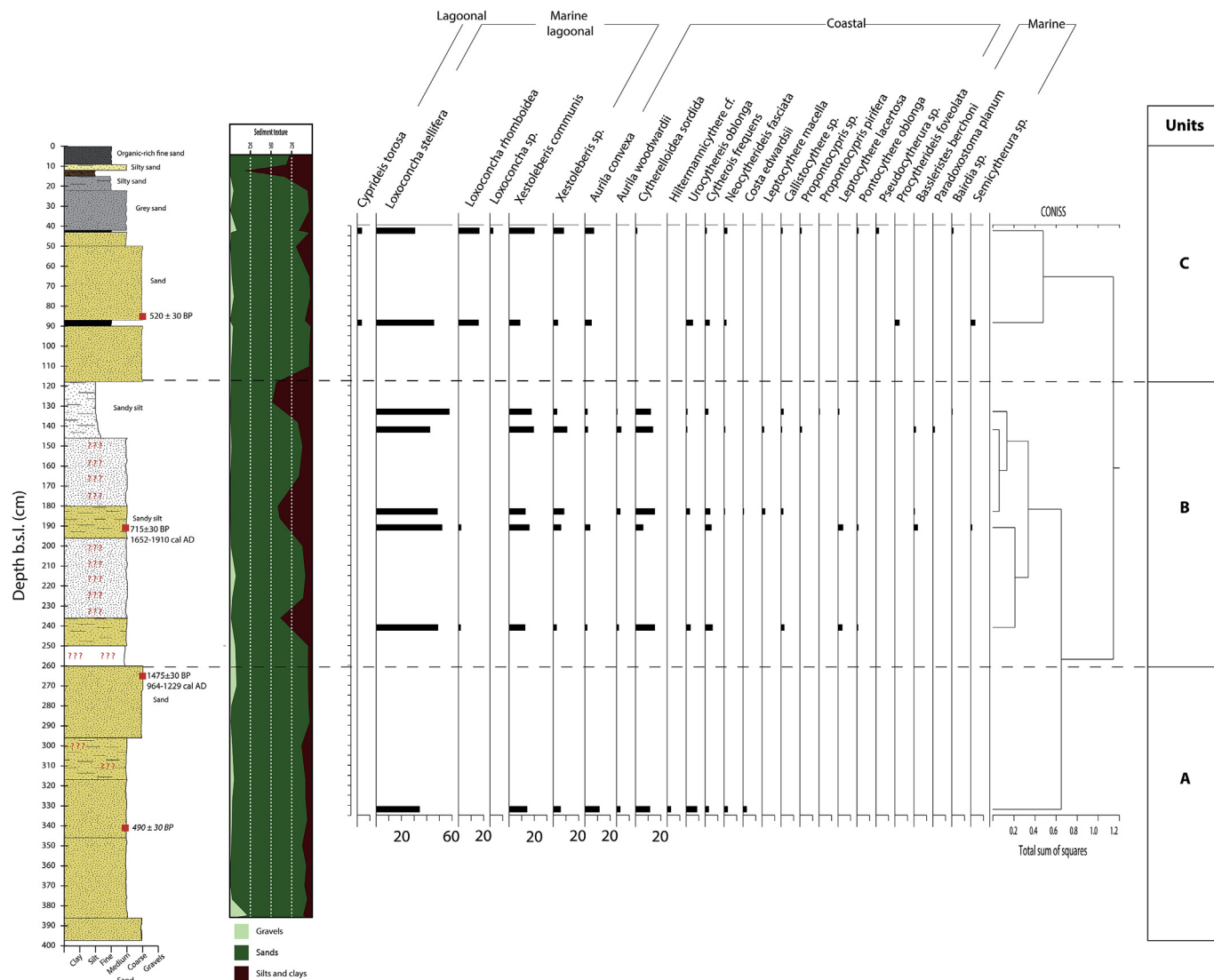


Fig. 4. Core POU2 stratigraphy and ostracods.

texture. The macrofauna (Fig. 3) is dominated by infralittoral sand assemblages (e.g. *Truncatella subcylindrica*, *Rissoa lineolate*, *Rissoa monodonta*, *Tricolia pullus*), hard substrate assemblages (e.g. *Conus mediterraneus*, *Gibbula* spp., *Jujubinus* sp., *Gibbula varia*, *Cythara paciniana*) and species living on algae. Ostracods are almost absent with the exception of a few coastal (45.7%) (*Aurilla convexa*, *Aurilla woodwardii*, *Cytherelloidea sordida*, *Hiltermannicythere* cf., *Urocythereis oblonga*, *Cytherois frequens*, *Neocytherideis fasciata*, *Costa edwardsii*) and marine lagoonal species (54.3%) (*Loxoconcha stellifera*, *Xestoleberis communis*, *Xestoleberis* sp.) at ~3.3 m depth (Fig. 4). This unit represents a shallow marine environment. Two marine shells were dated from the middle and the top of this unit (*Nassarius louisii* and *Cerithium vulgatum*, respectively; see Table 1), however, the deeper sample (490 ± 30 BP) yielded an age younger than the other shallower samples. The top of the unit was dated to 964–1229 cal AD (721–986 cal BP).

4.1.2. Unit B: leaky coastal lagoon

Unit B is found between 2.46 m and 1.18 m b.s.l., consisting of silty sand with *Posidonia oceanica* fibers and shell fragments. The unit presents a finer sedimentation towards the top. Gravels comprise 2.1% of the total sediment texture, sands 71.6% and silts-clays 26.3%. The macrofauna is dominated by lagoonal (*Loripes lacteus*, *Abra segmentum*),

upper muddy sand assemblages in sheltered areas (*Acanthocardia echinata*, *Cerithium vulgatum*), and infralittoral sand assemblages (*Tricolia pullus*, *Tricolia tenuis*, *Rissoa lineolate*, *Rissoa guerini*, *Mitra ebenus*). Microfossil assemblages are dominated by marine lagoonal (72.4%) (*Loxoconcha stellifera*, *Xestoleberis communis*) and coastal species (26%) (*Cytherelloidea sordida*). The middle of this unit was dated to 1652–1910 cal AD (40–298 cal BP). This unit is probably indicative of a leaky coastal lagoon, in constant connection with the sea (Kjerfve, 1994).

4.1.3. Unit C: lagoon periodically connected with the sea

Unit C is found from 1.18 m b.s.l. until the top of the core and consists of coarse to medium sand, which becomes siltier towards the top. The sands fraction represents 91% of the total sediment texture up to 50 cm depth and the proportion of silts-clays increases in the last 50 cm reaching 25.4%. Macrofauna analysis indicates that assemblages are poorer in terms of abundance and mainly consist of upper muddy sand assemblages in sheltered areas (*Cerithium vulgatum*), upper-clean sand assemblages (e.g. *Conus mediterraneus*, *Cardita calyculata*, *Gibbula* spp.), hard substrate species and algae. Ostracods are dominated by marine lagoonal species (75.6%) (e.g. *Loxoconcha stellifera*, *Xestoleberis communis*, *Loxoconcha rhomboides*); lagoonal species are represented by few individuals of *Cyprideis torosa* (3.5%), and coastal species (18.4%)

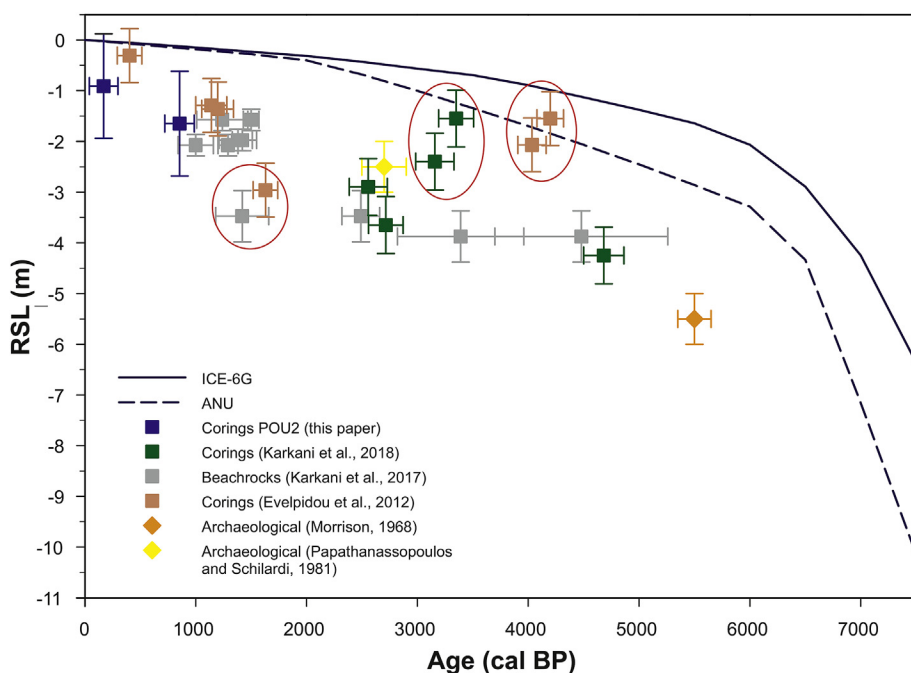


Fig. 5. Late Holocene RSL data from this study, compared with beachrock data from Karkani et al. (2017) and sediment corings from Paros (Karkani et al., 2018) and Naxos (Evelpidou et al., 2012). The circled samples are in disagreement with the rest of RSL index points. The RSL curves for Paros Island were obtained by numerically solving the Sea-Level Equation. The GIA models ICE-6G (solid) and ANU (dashed) have been employed.

(e.g. *Aurila convexa*, *Cytherelloidea sordida*, *Urocythereis oblonga*, *Cythereis frequens*). This unit is probably indicative of a lagoon more periodically connected with the sea (“choked lagoon” according to the classification of Kjerfve (1994). The middle of this unit was dated to 520 ± 30 BP.

5. Discussion

Most Cycladic islands are generally considered to be affected by a gradual subsidence, which is attributed to the crustal thinning, in an extensional tectonic regime (e.g. Mercier et al., 1989; Sakellariou and Tsampouraki-Kraounaki, 2019). The absence of morphological features indicative of uplift in the coastal zone, such as marine terraces or benches, elevated beachrocks, marine notches, or raised Quaternary coastal deposits are taken to substantiate this absence of local uplift. A subsidence regime has been noted by several authors for the wider study area (e.g. Desruelles et al., 2009; Lykousis, 2009; Evelpidou et al., 2012, 2014; Karkani et al., 2017).

The reconstructed RSL history from Paros and Naxos Islands is shown in Fig. 5. We included RSL estimates derived from archaeological data. In particular, according to Morrison (1968), a RSL rise of 5.5 m since 5500 BP may be estimated for Antiparos island, based on the Neolithic settlement of Saliagos. A RSL between -2 and -3 m around 2500–2900 BP has been estimated by Papathanassopoulos and Schilardi (1981), based on a number of archaeological findings around Paros Island (e.g. submerged moles, graves, buildings) (Fig. 5).

Overall, our new data support a RSL that rose by ~ 2 m in the last 2000 years, and by at least ~ 3.9 m since ~ 4500 years BP (Fig. 5). Conversely, two brackish samples from a core in Mikri Vigla (Naxos Island, Evelpidou et al., 2012), indicate that RSL reached ~ -2 m ± 0.5 at about ~ 4.0 ka. Similarly, two lagoonal samples from the Livadia core (Paros Island, Karkani et al., 2018) suggest a sea level between -1.5 and -2.5 m around 3100–3300 years BP. In both cases (Mikri Vigla and Livadia), the samples were rejected as they provided ages inconsistent with the chronostratigraphy.

In comparison with the modelled curves, which account for the effect of GIA, for Paros Island (Fig. 5), our RSL points have a lower position. To evaluate the tectonic component, we subtracted the elevation of the produced index points, from that of the corresponding points inferred from the GIA models at the same age (e.g. Chelli et al.,

2017). Average rates of tectonic subsidence were calculated for three different time frames (present to ~ 5500 cal BP, present day to 2500 cal BP, 2500 cal BP to 5500 cal BP), based on the mismatch between models and observations for Paros and the wider study area, considering the difference in elevation between sea level estimates from our data and from each of the models employed.

Since ~ 5500 cal BP, comparable tectonic subsidence rates ($\sim 1.0 \pm 0.4$ mm/yr) are found when the RSL data are corrected for the predictions of the two GIA models. The average rate of tectonic subsidence appears lower for the timespan 2500–5000 cal BP, being close to 0.7 ± 0.2 mm/yr, and higher ($\sim 1.2 \pm 0.4$ mm/yr) since 2500 cal BP. It appears evident from our findings that subsidence rates in the central Cyclades (Paros and Naxos) have not been constant since ~ 5500 cal BP. This suggests that, since ~ 2500 cal BP, the study area has been affected by seismic events that produced vertical displacements and/or during this time span the subsidence rate increased.

Evidence of seismic events, since about 3300 BP, have been reported in the study area by Evelpidou et al. (2014) through the analysis of submerged tidal notches, suggesting that at least part of the observed subsidence is related to vertical seismic displacements. Evelpidou et al. (2014) identified former shorelines at depths between 280 ± 20 and 30 ± 5 cm below modern sea level. In a recent study Vamvakaris et al. (2016), calculated the mean return period values for shallow earthquakes with $M > 6.0$ in the Aegean region and suggested very long return periods (> 200 years) for the broader Cyclades plateau, amongst other areas. The same authors also found that the most probable maximum magnitudes for a return period of 50 yr is expected to be less than $M = 5.0$, for low seismicity areas, such as the Cyclades islands plateau. In the Cyclades, one of the largest earthquakes in the last century occurred in July 1956, southwest of Amorgos Island, with a magnitude of 7.4, which was followed (a few minutes later) by a second of $M_s 7.2$ (e.g. Stiros et al., 1994; Okal et al., 2009; Brüstle et al., 2014).

For decades the Cycladic plateau has been considered as a tectonically inactive area (Sakellariou and Tsampouraki-Kraounaki, 2019). Our findings suggest that tectonic subsidence has contributed to the late Holocene evolution of the central Cyclades and it is most likely owed to a combination of seismic events and gradual long-term subsidence, due to the dominance of an extensional structural pattern. Furthermore, subsidence rates are higher than previously calculated for the study area (e.g. Pavlopoulos et al., 2011).

6. Conclusions

Our study focused on the reconstruction of RSL changes in the central Cyclades through the analysis of new and published sea-level data. We reevaluated the tectonic regime of the central Cyclades through the comparison of our data with new modelled RSL curves for Paros Island. Our findings suggest average tectonic subsidence rates close to 1 mm/yr since 5500 cal BP, which do not appear constant during the late Holocene; these values have increased since 2500 cal BP. The subsidence trend in the central Cyclades is most likely a combination of seismic events and gradual long-term subsidence, due to the dominance of an extensional structural pattern.

Acknowledgements

The authors would like to thank Alexandros Petropoulos, Giannis Saitis, Theophilos Valsamidis, Matina Seferli and Electra Kotopoulou for their help during fieldwork in Paros.

This work was co-funded by the General Secretariat for Research and Technology (1504) and the European Regional Development Fund, in the framework of the Bilateral project Greece – France entitled: ‘Sea level changes in Cyclades’.

This work has been partially carried out thanks to the support of the Labex OT-Med (ANR-11-LABX-0061) and of the A*MIDEX project (n° ANR-11-IDEX-0001-02), funded by the « Investissements d’Avenir » French Government program, managed by the French National Research Agency (ANR).

GS is funded by a FFABR (Finanziamento delle Attività Base di Ricerca) grant of the MIUR (Ministero dell’Istruzione, dell’Università e della Ricerca) and by a DiSpEA research grant.

References

- Bargnesi, E.A., Stockli, D.F., Mancktelow, N., Soukis, K., 2013. Miocene core complex development and coeval supradetachment basin evolution of Paros, Greece, insights from (U–Th)/He thermochronometry. *Tectonophysics* 595–596, 165–182. <https://doi.org/10.1016/j.tecto.2012.07.015>.
- Bradley, S.L., Milne, G.A., Horton, B.P., Zong, Y., 2016. Modelling sea level data from China and Malay-Thailand to estimate Holocene ice-volume equivalent sea level change. *Quat. Sci. Rev.* 137, 54–68. <https://doi.org/10.1016/j.quascirev.2016.02.002>.
- Brüster, A., Friederich, W., Meier, T., Gross, C., 2014. Focal mechanism and depth of the 1956 Amorgos twin earthquakes from waveform matching of analogue seismograms. *Solid Earth* 5, 1027–1044. <https://doi.org/10.5194/se-5-1027-2014>.
- Chelli, A., Pappalardo, M., Bini, M., Brückner, H., Neri, G., Neri, M., Spada, G., 2017. Assessing tectonic subsidence from estimates of Holocene relative sea-level change: An example from the NW Mediterranean (Magra Plain, Italy). *Holocene* 27 (12), 1988–1999. <https://doi.org/10.1177/0959683617715688>.
- Church, J.A., White, N.J., Aarup, T., Wilson, W.S., Woodworth, P.L., Domingues, C.M., Hunter, J.R., Lambeck, K., 2008. Understanding global sea levels: past, present and future. *Sustain. Sci.* 3, 9–22.
- d’Angelo, G., Gargiullo, S., 1978. Guida alle conchiglie Mediterranee. Fabbri Editori, Milano.
- Desruelles, S., Fouache, É., Ciner, A., Dalongeville, R., Pavlopoulos, K., Kosun, E., Coquinot, Y., Potdevin, J.-L., 2009. Beachrocks and sea level changes since Middle Holocene: Comparison between the insular group of Mykonos–Delos–Rhenia (Cyclades, Greece) and the southern coast of Turkey. *Glob. Planet. Chang.* 66, 19–33. <https://doi.org/10.1016/j.gloplacha.2008.07.009>.
- Doneddu, M., Trainito, E., 2005. Conchiglie del Mediterraneo. Il Castello. (Trezzano sul Naviglio).
- Engelhart, S.E., Horton, B.P., 2012. Holocene sea level database for the Atlantic coast of the United States. *Quat. Sci. Rev.* 54, 12–25.
- Engelhart, S.E., Horton, B.P., Douglas, B.C., Peltier, W.R., Horton, B.P., Tornqvist, T.E., 2009. Spatial variability of late Holocene and 20th century sea-level rise along the Atlantic coast of the United States. *Geology* 37, 1115–1118.
- Evelpidou, N., Pavlopoulos, K., Vassilopoulos, A., Triantafyllou, M., Vouvalidis, K., Syrides, G., 2012. Holocene palaeogeographical reconstruction of the western part of Naxos island (Greece). *Quat. Int.* 266, 81–93.
- Evelpidou, N., Melini, D., Pirazzoli, P., Vassilopoulos, A., 2014. Evidence of repeated Late Holocene subsidence in the SE Cyclades (Greece) deduced from submerged notches. *Int. J. Earth Sci.* 103 (1), 381–395. <https://doi.org/10.1007/s00531-013-0942-0>.
- Fontana, A., Vinci, G., Tascia, G., Mozzi, P., Vacchi, M., Bivi, G., Salvador, S., Rossato, S., Antonioli, F., Asioli, A., Bresolin, M., Di Mario, F., Hajdas, I., 2017. Lagoonal settlements and relative sea level during Bronze Age in Northern Adriatic: Geomorphological evidence and paleogeographic constraints. *Quat. Int.* 439, 17–36. <https://doi.org/10.1016/j.quaint.2016.12.038>.
- Gehrels, W.R., Woodworth, P.L., 2013. When did modern rates of sea-level rise start? *Glob. Planet. Chang.* 100, 263–277. <https://doi.org/10.1016/j.gloplacha.2012.10.020>.
- Hellenic Navy Hydrographic Service (HNHS), 2012. Statistical data for sea level of the Greek ports. HNHS, Athens (in Greek).
- Hijma, M.P., Engelhart, S.E., Tornqvist, T.E., Horton, B.P., Hu, P., Hill, D.F., 2015. A protocol for a geological sea-level database. In: Shennan, I., Long, A., Horton, B.P. (Eds.), *Handbook of Sea-Level Research*. Wiley, pp. 536–553. <https://doi.org/10.1002/9781118452547.ch34>.
- Horton, B.P., Shennan, I., 2009. Compaction of Holocene strata and the implications for relative sea level change on the east coast of England. *Geology* 37, 1083–1086.
- Kapsimalis, V., Pavlopoulos, K., Panagiotopoulos, I., Drakopoulou, P., Vandarakis, D., Sakelariou, D., Anagnostou, C., 2009. Geomorphological Challenges in the Cyclades Continental Shelf (Aegean Sea). *Z. Geomorphol.* 53 (Suppl. 1), 169–190.
- Karkani, A., Evelpidou, N., Vacchi, M., Morhange, C., Tsukamoto, S., Frechen, M., Maroukian, H., 2017. Tracking shoreline evolution in central Cyclades (Greece) using beachrocks. *Mar. Geol.* 388, 25–37. <https://doi.org/10.1016/j.margeo.2017.04.009>.
- Karkani, A., Evelpidou, N., Giaime, M., Marriner, N., Maroukian, H., Morhange, C., 2018. Late Holocene palaeogeographical evolution of Paroikia Bay (Paros Island, Greece). *Compt. Rendus Geosci.* 350 (5), 202–211. <https://doi.org/10.1016/j.crte.2018.04.004>.
- Kjerfve, B., 1994. Coastal Lagoons. In: Kjerfve, B. (Ed.), *Coastal Lagoon Processes*. Elsevier, pp. 1–8. [https://doi.org/10.1016/B978-0-444-01420-8\(01001-1\)](https://doi.org/10.1016/B978-0-444-01420-8(01001-1)).
- Lachenal, A.M., 1989. Écologie des ostracodes du domaine méditerranéen: application au Golfe de Gabès (Tunisie orientale). Les variations du niveau marin depuis 30 000 ans. *Doc. Lab. Geol. Lyon* 108, 1–239.
- Lambeck, K., Purcell, A., Johnston, P., Nakada, M., Yokoyama, Y., 2003. Water-load definition in the glacio-hydro-isostatic sea-level equation. *Quat. Sci. Rev.* 22 (2), 309–318.
- Lambeck, K., Antonioli, F., Purcell, A., Silenzi, S., 2004. Sea-level change along the Italian coast for the past 10,000 yr. *Quat. Sci. Rev.* 23, 1567–1598.
- Lykousis, V., 2009. Sea-level changes and shelf break prograding sequences during the last 4000a in the Aegean margins: Subsidence rates and palaeogeographic implications. *Cont. Shelf Res.* 29, 2037–2044. <https://doi.org/10.1016/j.csr.2008.11.005>.
- Mauz, B., Vacchi, M., Green, A., Hoffmann, G., Cooper, A., 2015. Beachrock: A tool for reconstructing relative sea level in the far-field. *Mar. Geol.* 362, 1–16. <https://doi.org/10.1016/j.margeo.2015.01.009>.
- Melis, R.T., Depalmas, A., Di Rita, F., Montis, F., Vacchi, M., 2017. Mid to late Holocene environmental changes along the coast of western Sardinia (Mediterranean Sea). *Glob. Planet. Chang.* 155, 29–41. <https://doi.org/10.1016/j.gloplacha.2017.06.001>.
- Melis, R.T., Di Rita, F., French, C., Marriner, N., Montis, F., Serrelli, G., Sulas, F., Vacchi, M., 2018. 8000 years of coastal changes on a western Mediterranean island: A multiproxy approach from the Posada plain of Sardinia. *Mar. Geol.* 403, 93–108. <https://doi.org/10.1016/j.margeo.2018.05.004>.
- Mercier, J.-L., Sorel, D., Vergely, P., Simeakis, K., 1989. Extensional tectonic regimes in the Aegean basins during the Cenozoic. *Basin Res.* 2, 49–71.
- Milne, G.A., Long, A.J., Bassett, S.E., 2005. Modelling Holocene relative sea-level observations from the Caribbean and South America. *Quat. Sci. Rev.* 24, 1183–1202.
- Morrison, I.A., 1968. Appendix I. Relative sea-level change in the Saliagos area since Neolithic times. In: Evans, J.D., Renfrew, C. (Eds.), *Excavations at Saliagos Near Antiparos*. Thames and Hudson, London, pp. 92–98.
- Nachite, D., Rodríguez-Lázaro, J., Martín-Rubio, M., Pascual, A., Bekkali, R., 2010. Distribution and ecology of recent ostracods from the Tahadart estuary (NW Morocco). *Rev. Micropaleontol.* 53, 3–15.
- Okal, E., Synolakis, C., Uslu, B., Kalligeris, N., Voukoulalas, E., 2009. The 1956 earthquake and tsunami in Amorgos, Greece. *Geophys. J. Int.* 178, 1533–1554.
- Papanikolaou, D., 1996. Geological map of Paros, scale 1:50000. IGME, Athens (in Greek).
- Papathanassopoulos, G., Schilardi, D., 1981. An underwater survey of Paros, Greece: 1979. Preliminary report. *Int. J. Naut. Archaeol. Underw. Explor.* 10 (2), 133–144.
- Papazachos, B.C., 1990. Seismicity of the Aegean and surrounding area. *Tectonophysics* 178, 287–308. [https://doi.org/10.1016/0040-1951\(90\)90155-2](https://doi.org/10.1016/0040-1951(90)90155-2).
- Pavlopoulos, K., Kapsimalis, V., Theodorakopoulou, K., Panagiotopoulos, I.P., 2011. Vertical displacement trends in the Aegean coastal zone (NE Mediterranean) during the Holocene assessed by geo-archaeological data. *Holocene* 22 (6), 717–728.
- Peltier, W.R., 2002. On eustatic sea level history: Last Glacial Maximum to Holocene. *Quat. Sci. Rev.* 21, 377–396.
- Peltier, W.R., 2004. Global glacial isostasy and the surface of the ice-age earth: the ice-5G (VM2) model and grace. *Annu. Rev. Earth Planet Sci.* 32, 111–149.
- Peltier, W.R., Argus, D.F., Drummond, R., 2015. Space geodesy constrains ice age terminal deglaciation: the global ICE-6G-C (VM5a) model. *Journal of Geophysical Research B: Solid Earth* 120 (1), 450–487. <https://doi.org/10.1002/2014JB011176>.
- Péres, J.-M., 1982. Major benthic assemblages. In: Kinne, O. (Ed.), *Marine Ecology*. Wiley, Chichester, pp. 373–522.
- Péres, J.-M., Picard, J., 1964. Nouveau manuel de bionomie benthique de la mer Méditerranée. *Periplus*, Marseille 137 pp.
- Pirazzoli, P.A., 2005. A review of possible eustatic, isostatic and tectonic contributions in eight late-Holocene relative sea-level histories from the Mediterranean area. *Quat. Sci. Rev.* 24 (18–19), 1989–2001. <https://doi.org/10.1016/j.quascirev.2004.06.026>.
- Reimer, P.J., McCormac, F.G., 2002. Marine radiocarbon reservoir corrections for the Mediterranean and Aegean Seas. *Radiocarbon* 44, 159–166.
- Reimer, P.J., Bard, E., Bayliss, A., Beck, J.W., Blackwell, P.G., Bronk Ramsey, C., Buck, C.E., Cheng, H., Edwards, R.L., Friedrich, M., Grootes, P.M., Guilderson, T.P., Hafliðason, H., Hajdas, I., Hatté, C., Heaton, T.J., Hoffmann, D.L., Hogg, A.G.,

- Hughen, K.A., Kaiser, K.F., Kromer, B., Manning, S.W., Niu, M., Reimer, R.W., Richards, D.A., Scott, E.M., Southon, J.R., Staff, R.A., Turney, C.S.M., van der Plicht, J., 2013. IntCal13 and Marine13 radiocarbon age calibration curves 0–50,000 years cal BP. *Radiocarbon* 55 (4), 1869–1887.
- Rovere, A., Stocchi, P., Vacchi, M., 2016. Eustatic and Relative Sea Level Changes. *Current Climate Change Reports* 2, 221–231. <https://doi.org/10.1007/s40641-016-0045-7>.
- Rovere, A., Furlani, S., Benjamin, J., Fontana, A., Antonioli, F., 2012. MEDFLOOD project: MEDiterranean sea-level change and projection for future FLOODing. *Alpine and Mediterranean Quaternary* 25, 3–5.
- Sakellariou, D., Galanidou, N., 2016. Pleistocene submerged landscapes and Palaeolithic archaeology in the tectonically active Aegean region, vol. 411. Geological Society of London, Special Publication, pp. 145–178. <https://doi.org/10.1144/SP411.9>.
- Sakellariou, D., Tsampouraki-Kraounaki, K., 2019. Plio-Quaternary Extension and Strike-Slip Tectonics in the Aegean. In: Duarte, J. (Ed.), *Transform Plate Boundaries and Fracture Zones*. Elsevier, pp. 339–374. <https://doi.org/10.1016/B978-0-12-812064-4.00014-1>.
- Salel, T., Bruneton, H., Lefèvre, D., 2016. Ostracods and environmental variability in lagoons and deltas along the north-western Mediterranean coast (Gulf of Lions, France and Ebro delta, Spain). *Rev. Micropaleontol.* 59 (4), 425–444.
- Sivan, D., Wdowinski, S., Lambeck, K., Galili, E., Raban, A., 2001. Holocene sea-level changes along the Mediterranean coast of Israel, based on archaeological observations and numerical model. *Palaeogeogr. Palaeoclimatol. Palaeoecol.* 167 (1–2), 101–117. [https://doi.org/10.1016/S0031-0182\(00\)00234-0](https://doi.org/10.1016/S0031-0182(00)00234-0).
- Sivan, D., Lambeck, K., Toueg, R., Raban, A., Porath, Y., Shirman, B., 2004. Ancient coastal wells of Caesarea Maritima, Israel, an indicator for relative sea level changes during the last 2000 years. *Earth Planet. Sci. Lett.* 222, 315–330. <https://doi.org/10.1016/j.epsl.2004.02.007>.
- Spada, G., Stocchi, P., 2007. SELEN: a Fortran 90 program for solving the “Sea level equation”. *Comput. Geosci.* 33 (4), 538–562.
- Stiros, S.C., Marangou, L., Arnold, M., 1994. Quaternary uplift and tilting of Amorgos Island (southern Aegean) and the 1956 earthquake. *Earth Planet. Sci. Lett.* 128 (3–4), 65–76.
- Stiros, S.C., Laborel, J., Laborel-Deguen, F., Morhange, C., 2011. Quaternary and Holocene coastal uplift in Ikaria Island, Aegean Sea. *Geodin. Acta* 24 (3–4), 123–131. <https://doi.org/10.3166/ga.24.123-131>.
- Stuiver, M., Reimer, P.J., Reimer, R.W., 2016. CALIB 7.1. [WWW program] at. <http://calib.org>, Accessed date: 4 December 2016.
- Teatini, P., Tosi, L., Strozzi, T., 2011. Quantitative evidence that compaction of Holocene sediments drives the present land subsidence of the Po Delta, Italy. *J. Geophys. Res. Solid Earth* 116 (B8). <https://doi.org/10.1029/2010JB008122>.
- Tirel, C., Gueydan, F., Tiberi, C., Brun, J.P., 2004. Aegean crustal thickness inferred from gravity inversion. Geodynamical implications. *Earth Planet. Sci. Lett.* 228, 267–280. <https://doi.org/10.1016/j.epsl.2004.10.023>.
- Vacchi, M., Marriner, N., Morhange, C., Spada, G., Fontana, A., Rovere, A., 2016. Multiproxy assessment of Holocene relative sea-level changes in the western Mediterranean: Sea-level variability and improvements in the definition of the isostatic signal. *Earth Sci. Rev.* 155, 172–197. <https://doi.org/10.1016/j.earscirev.2016.02.002>.
- Vacchi, M., Ghilardi, M., Spada, G., Currás, A., Robresco, S., 2017. New insights into the sea-level evolution in Corsica (NW Mediterranean) since the late Neolithic. *J. Archaeol. Sci.: Report* 12, 782–793. <https://doi.org/10.1016/j.jasrep.2016.07.006>.
- Vacchi, M., Ghilardi, M., Melis, R.T., Spada, G., Giaime, M., Marriner, N., Lorscheid, T., Morhange, C., Burjachs, F., Rovere, A., 2018. New relative sea-level insights into the isostatic history of the Western Mediterranean. *Quat. Sci. Rev.* 201, 396–408. <https://doi.org/10.1016/J.QUASCIREV.2018.10.025>.
- Vamvakaris, D.A., Papazachos, C.B., Papaioannou, C.A., Scordilis, E.M., Karakaisis, G.F., 2016. A detailed seismic zonation model for shallow earthquakes in the broader Aegean area. *Nat. Hazards Earth Syst. Sci.* 16, 55–84. <https://doi.org/10.5194/nhess-16-55-2016>.
- Van De Plassche, O., Wright, A.J., Horton, B.P., Engelhart, S.E., Kemp, A.C., Mallinson, D., Kopp, R.E., 2014. Estimating tectonic uplift of the Cape Fear Arch (south-eastern United States) using reconstructions of Holocene relative sea level. *J. Quat. Sci.* 29 (8), 749–759. <https://doi.org/10.1002/jqs.2746>.
- Woodroffe, S.A., Long, A.J., Milne, G.A., Bryant, C.L., Thomas, A.L., 2015. New constraints on late Holocene eustatic sea-level changes from Mahé, Seychelles. *Quat. Sci. Rev.* 115, 1–16. <https://doi.org/10.1016/J.QUASCIREV.2015.02.011>.